Electromagnetic modeling and optimization of photoconductive switches for terahertz generation and photocurrent transient spectroscopy

Heinrich DIESINGER[#1], Majid PANAHANDEH-FARD[#2], Dominique BAILLARGEAT[#1], Cesare SOCI[#1,#2,#3]

[#1]CINTRA CNRS/NTU/THALES, UMI 3288, Singapore
[#2]Division of Physics and Applied Physics, Nanyang Technological University, Singapore
[#3]Division of Microelectronics, Nanyang Technological University, Singapore

Abstract— **The frequency response of photoconductive switches critically determines the performance of terahertz generating photoconductive antennas and of fast photocurrent measurements. Width and shape of the electrical transient depend on both the photoconducting material and on the geometry of the switch. In this work, the response of the photoconductive switch is described by a hybrid model based on the intrinsic response of the active material and the electromagnetic model of the switch geometry. The transmission line with its gap is expressed in terms of transconductance. Hence, its response can be optimized with respect to bandwidth, and moreover be taken into account by deconvolving the transconductance transient from the measured transient to determine more accurately the intrinsic properties of the active material. The method is illustrated for photoconductive switches with organic semiconductors as the active material. Incompatible with standard lithographic techniques, photoconductive switches based on organic semiconductors are typically embedded in microstrip lines and have feature size limitations imposed by the electrode deposition technique. An alternative structure with coplanar access is shown to have a bandwidth greater than 70 GHz, which is almost one order of magnitude higher than the state of the art.**

Keywords — photoconductive switch; terahertz spectroscopy; picosecond transient photocurrent; microstrip line; coplanar line; organic photoconductors

I. INTRODUCTION

Terahertz spectroscopy has applications in molecular and biochemical sensing due to signatures of many molecules in this part of the spectrum, as well as in imaging for security and defense since many materials are transparent at these wavelengths [1]. Photoconductive switches are currently used for THz generation to produce a continuous spectrum up to some THz in the form of a photocurrent transient upon exposure to an ultrashort laser pulse. Photoconductive switches may be part of a setup using the electric transient to characterize a third component or material, or the active material within the switch may be the object of interest. In order to fabricate performant photoconductive switches, different approaches can be followed and combined. The first device presented by Auston used two consecutive laser pulses of different wavelenghts to first generate a short-circuit across a gap in a microstrip and send a wavefront from the pre-biased portion to the other side of the gap, then short-circuit the stripline to ground to turn off the switch and hence define the end of the pulse [2]. Thereby, pulses much shorter than the photocarrier lifetime could be obtained. Later works concentrated on designing materials having a short intrinsic carrier lifetime by methods such as radiation damage [3], amorphization [4], and by MBE growth (low temperature grown GaAs and advanced composite materials containing nitrogen and antimony) [5]. Alternatively, short carrier lifetime can also be achieved by rapidly extracting the carriers in a narrow gap under high bias.

In the field of organic semiconductors, the analysis of the photocurrent transient with sub-nanosecond time resolution has been extensively used to obtain fundamental information about the carrier dynamics of the active material such as polaron photogeneration, thermalization, trapping and recombination [6]. It is noteworthy that the comprehension of carrier dynamics in the sub-nanosecond range is crucial for devices working at steady-state, in particular polymer photovoltaics featuring bulk heterojunction materials, since competing processes occurring immediately after photocarrier generation have a tremendous effect on their efficiency [7]. Material engineering focuses on optimizing the inherent properties of polymer blends aimed at optimizing the rate of photocarriers separation and improving solar cell efficiency.

Whether the photoconductive switch is used for terahertz generation to study other components placed on a transmission line or by generating free-space terahertz radiation by an antenna, or it is used to characterize the active material of the switch, both applications are subject to the response of the active material and the response of the switch consisting of the electrodes and the transmission line access. The objective of this work is to develop a hybrid model allowing to decompose the characteristics of the switch into the response of the material and the response due to the transmission line geometry. Consequently, the geometry can be optimized to better approach the intrinsic response of the photoconducting material, and simultaneously the modeled response of the transmission line structure can be deconvolved from the experimentally observed transient to derive the intrinsic properties of the photoconductive material.

Research partially supported by the Funding of Initiatives in Support of NTU 2015. M.P.F. acknowledges financial support from the Yousef Jameel Scholarship Fund.

978-1-61284-718-4/11/$26.00 ©2011 IEEE

II. CONDITIONS AND REQUIREMENTS FOR THE MODEL

Since the intrinsic properties of the gap material are in the focus of the work, the model must provide for the temporal response of the active material. It is assumed that the length of the ultrashort laser pulse is negligible to the material response and can be treated as a Dirac peak. The frequency response of a photoconductive switch has previously been studied as function of the frequency of the applied bias [8].

However, here the focus is on photoconductive switches where transients are generated under DC bias. Furthermore, it shall be assumed that the applied bias is large compared to the amplitude of the generated transient. Therefore, the frequency dependence with respect to the bias is not required for describing the material.

In another work, the active zone had been described as S-matrix [9]. This description introduces frequency dependence with respect to bias, and additional frequency dependence had been introduced to take into account the response with respect to the incident light. However, the S-matrix description is valid only for linear bias dependence.

Since this work focuses on the temporal response of the active material under DC bias, the model discussed in the following is based on describing the active region as a current generator. It allows taking into account non-linear effects by studying different DC bias case by case. Phenomena that lead to a non-linear bias dependence include the enhancement of dynamics of the switch by fast carrier sweepout [10, 11] or field-assisted charge carrier photogeneration [12].

The frequency behavior of the surrounding structure is modeled as S-matrix by applying electromagnetic methodology instead of the lumped element descriptions adopted in previous works.

III. ELECTROMAGNETIC MODEL OF THE SWITCH

The photoconductive switches considered in this study are schematically described in Fig. 1. In general, the active material is represented by a current generator. The surrounding structure transmits a wave propagating towards the load Z_L upon generation of a current transient. Both configurations are suitable for fabrication on organic semiconductors without any direct lithography on the active material. Panel (a) shows the microstrip line conventionally used for the study of conjugated polymers or molecular crystals [13]. The switch in panel (b) contains a transition from microstrip to coplanar access terminals and its design is currently under study to increase the bandwidth of organic photoconductive switches. This geometry is conventionally used for microwave switches [14, 15].

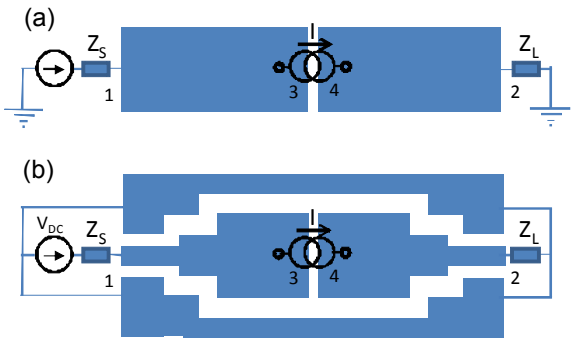

Figure 1. Photoconductive switches comprised of an active material described by a current generator, and surrounding transmission line structures; (a) standard gap in microstrip line; (b) structure containing a transition to coplanar accesses. Bias is applied by a voltage source with idle voltage V_{DC} and source impedance Z_S. The structure transforms the generated photocurrent into a transient wave propagating towards the load Z_L.

In contrast to the active material, the response of the transmission line structure can be adequately described by an S-matrix since nonlinear behavior with respect to voltage is not expected. The RF coupling across the gap has an effect on the conversion of the photocurrent into a propagating wave towards the load. Previous works have approached the gap as a capacitor and derived a lowpass behavior with a time constant,

$$\tau = 1/Z_L C_{Gap}. \qquad (1)$$

However, the geometry of the capacitor cannot be accounted by a plane capacitor model. Furthermore, the lumped element approach is not expected to yield a good description of the entire electromagnetic coupling between the portions of waveguide on both sides of the gap: the transmission line interrupted by a gap can be considered as two pieces of transmission line facing each other. Since the cross-section of the transmission line is small with respect to the wavelength, an open ended transmission line can be expected to emit an evanescent wave with a decay length on the order of the lateral dimension of the waveguide. Therefore, the coupling between the transmission lines on each side of the gap will be calculated rigorously by including a portion of transmission line into the electromagnetic modeling by full electromagnetic simulation using Ansoft HFSS [16]. As a first indication on the choice of the computational volume of the electromagnetic simulation of the device, a length of twice the substrate thickness into each portion of transmission line should provide a good description of the electromagnetic coupling. On the other hand, we would also like to include the transition from microstrip to coplanar waveguide in the computation for the structure of Fig. 1 (b). If the computational volume is extended to a length significantly larger than the gap, the description of the gap and accesses as 2-port device becomes inaccurate because the current generator would then act on the access ports at the extremities of the microstrip rather than on the strip edges near the gap where the current is essentially collected. We therefore suggest describing the structure as a 4-port S-matrix. The assignment of port numbers is indicated in

Fig. 1: the current generator is applied to the inner ports labeled 3 and 4. Adding ports 3 and 4 and terminating them with infinite impedance according to the description of the active material as current generator should not change the coupling between port 1 and 2 [*1].

The resulting equivalent circuit is shown in Fig. 2 (a). The current generator between ports 3 and 4 has been replaced by two current generators applying opposite currents on the ports.

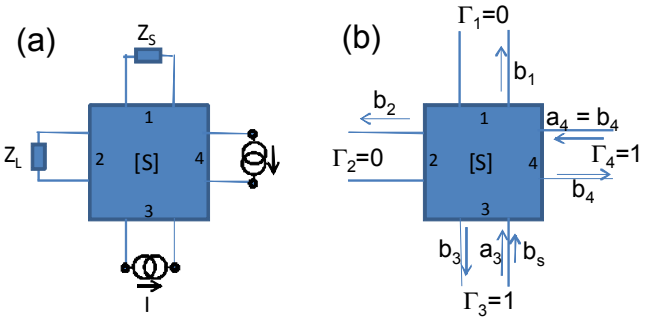

Figure 2. S-matrix description of the photoconductive switch: (a) equivalent circuit representing the transmission lines as 4-port S-matrix and the active area as a current generators; (b) schematic of power waves for the application of a current on port 3: incident wave b_s, incident and outgoing waves a_n and b_n, in particular b_2 transmitted to the output, for the particular boundary conditions.

The next step consists in deriving the ratio between a power wave b_s incident on port 3 and the outgoing wave b_2 on port 2. This will be repeated for b_s incident on port 4 and superposed.

In contrast to power transducer gain where the steady state including multiple internal reflections between a source and a load is calculated, for the transient analysis we will not include reflection from the DC bias applied to port 1 and the oscilloscope to port 2. Either the bias is applied by a source with internal impedance Z_0 and the oscilloscope has Z_0 impedance, or otherwise the mismatches are at least far enough from the photoconductive and connected via a Z_0 cable, so that reflection from them will be clearly distinguishable from the original transient. Therefore, there is no incident wave on ports 1 and 2.

On the other hand, since in a first approach the round trip time in the computational volume (2 mm length) can still be considered small compared to the length of the resulting transient, we adopt the standard procedure used in transducer gain calculation that takes into account multiple reflections within the 4-port device. In particular, on the open-circuited ports 3 and 4, we establish the steady-state for an infinite number of internal reflections.

A conflict occurs for multiple internal reflections on the portions of lines in the computational volume: making the computational volume longer leads to including multiple internal reflections that have too much delay to contribute to the original transient. The conflict is resolved by designing the structure such that S_{11} and S_{22} are close to zero.

For the 7 power waves indicated in Fig. 2 (b), 6 linear equations are established, allowing to resolve for a relation between b_2 and b_s. Eliminating directly a_4 and a_3 by taking into account the total reflection at the open circuits simplifies the solution of the equation system and gives the same result as solving 6 equations for 7 unknown power waves and applying the total reflections on ports 3 and 4 afterwards.

Including these conditions, we obtain

$$\frac{b_2}{b_s} = \frac{S_{23}(1-S_{44}) + S_{24}S_{43}}{(1-S_{44})(1-S_{33}) - S_{34}S_{43}} \qquad (2)$$

for the wave on output port 4 as function of source wave b_s. The reasoning is repeated for a wave b_s incident on port 4.

The incident power waves are replaced by

$$b_s = I\sqrt{Z_0} \qquad (3)$$

and the voltage on the Z_0 output line propagating toward the oscilloscope is

$$v_2 = b_2\sqrt{Z_0}\,. \qquad (4)$$

By superposing the contributions of both current generators, taking further into account the reciprocity ($S_{ij} = S_{ji}$) and symmetry (e.g. $S_{33} = S_{44}$, $S_{11}=S_{22}$) and expressing the incident wave as function of the current, we obtain:

$$v_2 = IZ_0\frac{S_{31} - S_{41}}{1 - S_{33} + S_{34}}\,. \qquad (5)$$

IV. Results on the Transient Response of the Transmission Line Structure

The transimpedance v_2 / I is finally Fourier-transformed to obtain the transient response of the transmission line structure. The resulting transient responses for the microstrip structure and for the structure containing the transition to coplanar access are shown in Fig. 3(a) and 3(b), respectively.

*1: *S21'* can be calculated as function of the 4x4 S matrix by applying open circuit boundary conditions to ports 3 and 4. Comparison with *S21* for the same structure modeled without ports 3 and 4 showed good agreement.

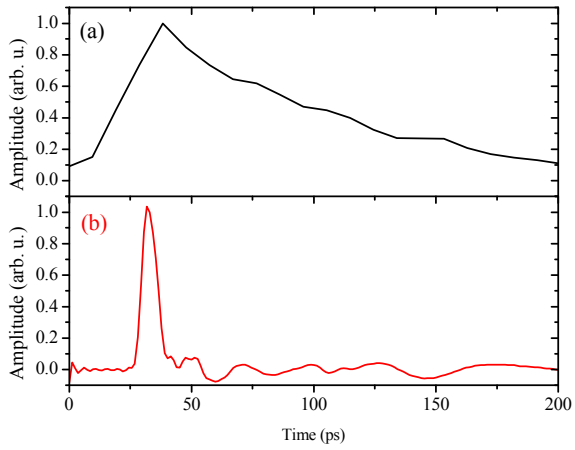

Figure 4. Transient response of the transmission line structures of Fig. 1. To facilitate comparison, the peak amplitude has been normalized to 1; (a) microstrip structure of Fig. 1 (a); a decay time constant of about 200 ps is observed; (b) structure with coplanar accesses of Fig. 1(b); a peak width of about 20 ps is observed.

The response of the microstrip line is an exponential decay with a time constant of about 200 ps. However, for the switch with coplanar accesses, a peak of about 20 ps width is obtained.

V. CONCLUSION

Modeling and simulations presented here evidence the contribution of the transmission line structure including coplanar access to enhance the response of the switch. A performance increase of about one order of magnitude is therefore obtained by introducing the coplanar accesses. Besides increasing bandwidth, knowing the response of the transmission line will also allow deconvolving it from measurement data to obtain the intrinsic photoconductive response of the active material.

In the future, the optimization of the structure will be further refined and the deconvolution will be applied to experimentally acquired transients observed by a 70 GHz sampling oscilloscope.

ACKNOWLEDGEMENT

M.P. would like to acknowledge financial support (scholarship and funding) from a Yousef Jameel grant.

REFERENCES

[1] Aniruddha S. Weling and David H. Auston, "Novel sources and detectors for coherent tunable narrow-band terahertz radiation in free space," J. Opt. Soc. Am. B, Vol. 13, pp. 2783-2791, December 1996.

[2] D. H. Auston, "Picosecond optoelectronic switching and gating in silicon," Appl. Phys. Lett., Vol. 26, pp.101-103, February 1975.

[3] P. R. Smith, D. H. Auston, A. M. Johnson, and W. M. Augustyniak, "Picosecond photoconductivity in radiation-damaged silicon-on-sapphire films," Appl. Phys. Lett., Vol. 38, pp.47-50, January 1981.

[4] D. H. Auston, P. Lavallard, N. Sol, and D. Kaplan, "An amorphous silicon photodetector for picosecond pulses," Appl. Phys. Lett., Vol. 36, pp. 66-68, January 1980.

[5] F. W. Smith, H. Q. Le, V. Diadiuk, M. A. Hollis, A. R. Calawa, S. Gupta, M. Frankel, D. R. Dykaar, G. A. Mourou, and T. Y. Hsiang, "Picosecond GaAs-based photoconductive optoelectronic detectors," Appl. Phys. Lett., Vol. 54, pp. 890-892, March 1989.

[6] M. B. Sinclair, D. Mcbranch, T. W. Hagler, A. J. Heeger, "Subpicosecond photoinduced absorption in poly[2,5-thienylene vinylene] and poly[3-methoxy-6-(2-ethyl-hexyloxy) phenylene vinylene]," Synthetic Metals Vol. 50, pp. 593-602, August 1992

[7] C. Soci, I. W. Hwang, D. Moses, et al., "Photoconductivity of a low-bandgap conjugated polymer," Adv. Funct. Mater., Vol. 17, pp. 632-636, March 2007.

[8] J. F. Roux, J. M. Delord, J. L. Coutaz, "RF Frequency Response of Photoconductive Samplers," IEEE J. Quantum Electron., Vol. 47, pp. 223-229, February 2011.

[9] K. Green, R. Sobolewski, "Extending scattering-parameter approach to characterization of linear time-varying microwave devices, IEEE Trans. Microwave Theory Tech., Vol. 48, pp 1725-1731, October 2000.

[10] D. Moses, M. Sinclair, A. J. Heeger, "carrier photogeneration and mobility in polydiacetylene - fast transient photoconductivity," Phys. Rev. Lett. Vol. 58, pp. 2710-2713, June 1987.

[11] Z. Xu, S. F. Yoon, W. K. Loke, et al., "Design Considerations for 1.3 mu m GaNAsSb-GaAs High Speed and High Quantum Efficiency Waveguide Photodetectors," J. Lightwave Technol. Vol. 27, pp. 2518-2524, July 2009.

[12] D. Moses, J. Wang, A. J. Heeger, N. Kirova, S. Brazovski, "Singlet exciton binding energy in poly(phenylene vinylene," Proc. Natl. Acad. Sci. U.S.A. Vol. 98, pp. 13496-13500, November 2001.

[13] D. Moses, C. Soci, X. L. Chi, et al., "Mechanism of carrier photogeneration and carrier transport in molecular crystal tetracene," Phys. Rev. Lett., Vol. 97, pp. 067401, August 2006.

[14] F. A. Hegmann, D. Jacobs-Perkins and C.-C. Wang, S. H. Moffat, R. A. Hughes, and J. S. Preston, M. Currie, P. M. Fauchet, T. Y. Hsiang, and Roman Sobolewski, "Electro-optic sampling of 1.5-ps photoresponse signal from YBa2Cu3O72d thin films," Appl. Phys. Lett. Vol. 67, pp. 285-287, July 1995.

[15] V. J. Logeeswaran, A. Sarkar, M. S. Islam, "A 14-ps full width at half maximum high-speed photoconductor fabricated with intersecting InP nanowires on an amorphous surface," Appl. Phys. A Vol. 91, pp. 1-5, January 2008.

[16] http://www.ansoft.com